Journal of Nuclear Materials 466 (2015) 12–20

Contents lists available at ScienceDirect

Journal of Nuclear Materials

journal homepage: www.elsevier.com/locate/jnucmat

Review

A review on hydride precipitation in zirconium alloys

Jacob Bair [a], Mohsen Asle Zaeem [a, *], Michael Tonks [b]

[a] Missouri University of Science and Technology, 1400 N Bishop Ave., Rolla, MO 65409, USA
[b] Idaho National Laboratory, 2525 Fremont Ave., Idaho Falls, ID 83401, USA

ARTICLE INFO

Article history:
Received 29 January 2015
Received in revised form
30 June 2015
Accepted 8 July 2015
Available online 11 July 2015

ABSTRACT

Nucleation and formation of hydride precipitates in zirconium alloys have been an important factor in limiting the lifetime of nuclear fuel cladding for over 50 years. This review provides a concise summary of experimental and computational studies performed on hydride precipitation in zirconium alloys since the 1960's. Different computational models, including density functional theory, molecular dynamics, phase field, and finite element models applied to study hydride precipitation are reviewed, with specific consideration given to the phase field model, which has become a popular and powerful computational tool for modeling microstructure evolution. The strengths and weaknesses of these models are discussed in detail. An outline of potential future work in this area is discussed as well.

Contents

1. Introduction

Zirconium (Zr) and its alloys have been used in nuclear fuel claddings and pressure tubes for more than 50 years, because of their low neutron absorption, and good strength and corrosion resistance at high temperatures. Despite these desirable material properties, Zr alloys suffer from an important weakness. During operation in nuclear power plants and in the storage period after usage, the Zr claddings are constantly being water-cooled. Oxygen from the water bonds with the outer layer of the cladding to create Zr Oxides, releasing Hydrogen (H) atoms, some of which enter the cladding. When the H concentration surpasses the terminal solid solubility limit of the Zr, hydrides are formed which lead to embrittlement and fracture through delayed hydride cracking (DHC). Examples of hydride related failure have been outlined in detail in recent papers [1,2]. Because of these problems, significant research has been conducted over the past 60 years to better understand hydride formation and morphology. The objective of this paper is to provide a concise review of experimental research and computational modeling efforts completed to this point on the subject of Zr hydrides. A more exhaustive review on experimental works done to this point can be found in a book on hydrides by Puls [3].

* Corresponding author.
E-mail address: zaeem@mst.edu (M. Asle Zaeem).

http://dx.doi.org/10.1016/j.jnucmat.2015.07.014
0022-3115/

This review paper is organized as follows: in Section 2 a review on the experimental studies of Zr hydrides from the past 60 years is discussed; in Section 3 computational research is discussed, starting from the atomic scale (Density Functional Theory and Molecular Dynamics) and working up to mesoscale models (Finite Element Models and Phase Field Models); in Section 4 some conclusions are drawn which include potential research topics which may improve our understating of hydride precipitation in Zr alloys.

2. Experimental study of zirconium hydrides

There are four known hydride phases in the Zr–H system: $ZrH_{0.5}$-ζ, ZrH-γ, $ZrH_{1.5-1.7}$–δ, and ZrH_2-ε. The recently discovered ζ phase is metastable and is believed to be a transitional phase between α-Zr and δ or γ hydrides [4]. Previous speculations on the potential existence of the fourth phase (ζ phase) can be found in Refs. [5,6] by Bailey and Carpenter. Zhao et al. [4] hypothesized that the new phase may play an important role in the stress-reorientation of hydrides. Several experimental studies have been performed to create an accurate phase diagram of the Zr–H system [7–15]. The ζ phase is not included in any phase diagram because it is metastable. Since the early 1960's, the stability or metastability of the γ phase has been debated [15–21], and some early phase diagrams contained the γ hydride phase. Most current works agree that the γ hydride phase is indeed a metastable phase that is stable only under certain conditions [19–21]. The stability of γ hydrides is discussed in detail in Section 2.2. Most experimental work has been done on the γ and δ phases, which are most commonly credited with mechanical failures of claddings. In the following subsections important results of experimental studies related to Zr hydrides and their effects on nuclear fuel rod claddings are discussed.

2.1. Solubility and absorption of hydrogen in zirconium

Due to losses in ductility and other negative effects of hydrides, many experiments have been done to determine the Terminal Solid Solubility (TSS) of H in Zr [2,22–28]. The TSS is different for precipitation and dissolution of hydrides, so there are several papers that distinguish them by TSSP and TSSD, respectively. Solubility of H is important because hydrides can only precipitate after the solubility limit is surpassed. According to a review by Ells in 1968, the solubility of H drops drastically with temperature, from about 50 at% H at 500 °C to 0.7 at% H at 300 °C, and to around 10^{-4} at% H at 20 °C [29]. These values differ somewhat from those found by more recent studies, and the 50 at% H at 500 °C is most likely a typo in Ells' review paper, and is meant to be 5 at%. More recent studies still show a significant increase in solubility with temperature [24–30]. This increase in solubility shows the necessity of thoroughly understanding the TSSP and TSSD of H in Zr and its alloys. The results of previous experiments show that the TSSP changes very little due to alloying elements [22,23], applied stresses [25], and irradiation of the material [26]. However, Carpenter and Watters performed an *in situ* study of the dissolution of hydrides, and found that the TSSD may increase by irradiation [30]. Another work done by Cann and Atrens [28] shows that extrapolations of data found by others at high H concentrations is relatively accurate for lower H concentrations. Fig. 1 presents the results obtained by Une et al. [26] through Differential Scanning Calorimetry for TSS for precipitation and dissolution of hydrides in Zr. Their results compared very closely with experiments done through other methods, such as those in Refs. [24–30]. According to their equation, the solubility of H at 500 °C is around 5.6 at%, at 300 °C it is 1.5 at%, and at room temperature it is 0.01 at%.

Because of the importance of the amount of H in the system, there are some studies on determining the fraction of H absorbed into the Zr matrix during oxidation of the fuel claddings. The fraction of H absorbed by the claddings is related directly to the rate at which H concentration increases past the point of solid solubility. Couet et al. proposed a new technique for quantitatively determining H concentration in Zr alloys called cold neutron prompt gamma activation analysis [31]. They also recently showed that the ratio of H absorbed to total H generated in the corrosion reaction varies significantly with different alloying elements [32]. They found that Nb reduces H pickup while Cu increases it. It was also determined that coarser $ZrFe_2$ or $ZrCr_2$ precipitates reduce H pickup. In general, the fraction of absorbed H increases with exposure time. The results found by Couet et al. confirmed and expanded some previous studies [33–35]. These conclusions could become important in creating alloys which are more resistant to H pickup, resulting in less hydride formation and increasing the lifetime of claddings. For this reason, more research should be done to identify the factors that could reduce H absorption in the cladding materials; including the use of alloying elements or secondary precipitates that can potentially decrease H absorption. For example, finding the optimum amount of Nb and the optimum size of $Zr(Fe, Cr)_2$ precipitates that can provide the maximum protection against H absorption while maintaining sufficient mechanical properties, could be an important study which can help improving current cladding materials.

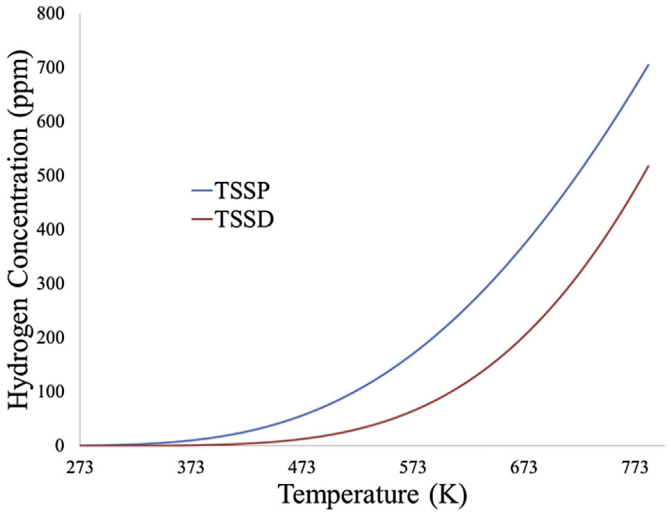

Fig. 1. Terminal solid solubility (TSS) of H in Zr by Une et al. [26]. They found very little differentiation between their studies and other experimental work in finding the terminal solubility of H in Zr.

2.2. Hydride crystallography

It has been shown by experiments that the four phases of Zr Hydrides have different crystal structures. δ hydride and ε hydride are stable Face-Centered Cubic (FCC) and Face-Centered Tetragonal (FCT) phases, respectively [4]. γ hydrides are FCT and ζ hydrides are trigonal. The majority of experimental studies done to date have been on δ and γ phases, since they are the phases most liable for embrittlement and fracture of materials. Although they differ in crystallography, both the δ and γ phases grow in similar directions within the Zr matrix. The direction of growth has been determined to be $[11\bar{2}0]$, but conflicting data has been collected on the habit planes. These hydride phases grow in the form of plates, and the broad side of the plate which is parallel to the crystallographic plane in α Zr is called the habit plane. Weatherly [36] found that γ hydrides form as acicular plates having $\{10\bar{1}0\}$ or $\{10\bar{1}L\}$ habit planes, where $L \approx 7$. Westlake [37] found that the preferred habit plane of an unspecified phase of hydride (probably δ from the

sample preparation) is $\{10\bar{1}7\}$ in Zircaloy 2 and 4, and it is $\{10\bar{1}0\}$ in pure Zr. Other possible δ hydride habit planes reported in the literature are $\{10\bar{1}2\}$, $\{11\bar{2}1\}$, and $\{11\bar{2}2\}$ [38], $\{10\bar{1}1\}$ [39], and the basal plane [40–45]. Singh et al. noted that temperature may have an important effect on which planes are the habit planes [41]. These discrepancies are briefly discussed by Kim et al. [46], speculating that DHC growth patterns and notch directions indicate that the $\{10\bar{1}7\}$ plane is the most probable habit plane.

The fraction of δ and γ hydrides is related to the H concentration and cooling rate of the Zr. A higher H concentration and/or a slower cooling rate will lead to production of more δ hydrides, and the opposite will lead to more γ hydrides [47–49]. The possibility of formation of each of these two hydride phases has also been linked to oxygen concentration by Cann et al. [50], who stated that higher amounts of oxygen impurity led to higher δ fractions, and low oxygen impurity favors γ hydrides. They also found that the hydrogenation technique, grain size, and prior heat treatments had no effect on the phase of the hydrides formed. Studies by several other researchers have indicated that γ hydrides may be a stable phase at temperatures below 250 °C [15–18], and a work by Root et al., in 2003 show that δ to γ phase transformation can occur very slowly at low temperatures [16]. However, in 2004, Lanzani and Ruch found that γ is a metastable phase at least in low purity Zr, and no δ to γ transformation could be obtained [20]. In a recent paper on the effects of yield strength on hydride phase stability, Tulk et al. [19] referenced several other studies that found γ to be a stable phase, but they realized that after heating to the H dissolution temperature, no δ to γ phase transformation could be observed [19,21], though they also found that the stability of the γ phase could be related to several factors related to the matrix material. Their observations would indicate that except under certain unknown conditions created in those experiments showing δ to γ phase transformation, the γ phase is indeed metastable. Due to the relatively slow cooling rates in the nuclear fuel rod claddings during operation, we can conclude that the δ hydride formation causes the majority of DHC under the actual operating conditions. However, it may still be important to understand if there are conditions under which γ hydrides become stable.

Therefore, continued research on possible temperature effects on habit planes and on conditions of stability of γ hydrides could both be useful in furthering the progress of understanding Zr hydrides and their effects on claddings. In their recent paper, Singh et al. stated that a study for investigating the effects of temperature was underway at that time, and could be completed in the near future [41]. The possibility of stability of γ hydrides under special conditions could be tested by attempting to recreate those experiments where the δ to γ phase transformation was observed and noting any differences in sample preparation. It appears that in the experiment by Root et al. the initial condition for the experiment involved nearly completely γ hydrides [16], which were then heated past the dissolution temperature and reprecipitated as δ hydrides. It is possible that dislocation loops and memory effect could have influenced the experiment to create the transformation from δ to γ or it may be some other factor, this should be investigated further.

2.3. Hydride growth and Re-orientation

It has been shown that hydrides tend to form preferentially along grain boundaries where grain boundaries are aligned with the habit plane of the hydrides [47,51,52]. Thus, grain boundary orientations seems to have a significant effect on whether or not intergranular hydrides form [52]. Experimental studies by Mani-Krishna et al. have suggested that using low Coincidence Site Lattice (CSL) boundaries can potentially reduce hydride precipitation [53,54]. Their findings also suggest that in Zr alloys with a β phase present, hydrides would preferentially precipitate on an α-β interface in the α matrix. It is also shown that externally applied stresses affect the direction of hydride growth, while without stresses, only the $[11\bar{2}0]$ directions are available for hydride growth, hydrides prefer to grow along the direction which is perpendicular to the tensile stress or parallel to compressive stress [36,55]. Puls [55] found that hydrides near a fracture surface were always oriented with plates perpendicular to the applied tensile stress. He also found that hydrides tend to fracture transversely, similar to findings of Beevers and Edmonds in 1969 [56]. Qin et al. suggest that solute segregation may be used to lower grain boundary energy and reduce the effect of grain boundaries on precipitation [57]. Their results also indicate that a stronger α Zr matrix would reduce precipitation along grain boundaries.

Hydride orientation plays an important role in the embrittlement of the cladding; radially oriented hydrides have been shown to be much more detrimental to mechanical properties than circumferentially oriented hydrides. Hydride reorientation becomes important during the transition of nuclear fuel rods between wet and dry storage; during this transition, many of the hydrides are dissolved into the matrix as the temperature rises above the dissolution temperature and then precipitate again upon cooling. Colas et al. [27,58] used *in situ* transmission diffraction experiments to find the hydride precipitation and dissolution temperatures, and also determine the generated stresses in re-orientation of hydrides; the data they obtained was again reasonably close to the results obtained through previous *ex situ* works. There is some memory effect believed to be caused by dislocation loops, which form during the initial phase change as seen in Fig. 2. These dislocation loops may be very important in whether the hydrides reorient or not during this transition [27,58–60]. Studies by Colas et al. have found threshold stresses for this reorientation [27,58,60,61]. Their results indicate that δ precipitates forming under no applied load are elastically strained in compression in both the rolling and transverse directions due to the lower density of hydrides. Under an applied load, they found that re-oriented δ hydrides start precipitating with high compression strains in the transverse direction. Their results also indicate a different strain state for re-oriented hydrides than that of circumferential hydrides. Another important finding of these experiments was a large effect of thermo-mechanical cycles on hydride re-orientation. As the number of cycles increased, the fraction of re-oriented hydrides greatly

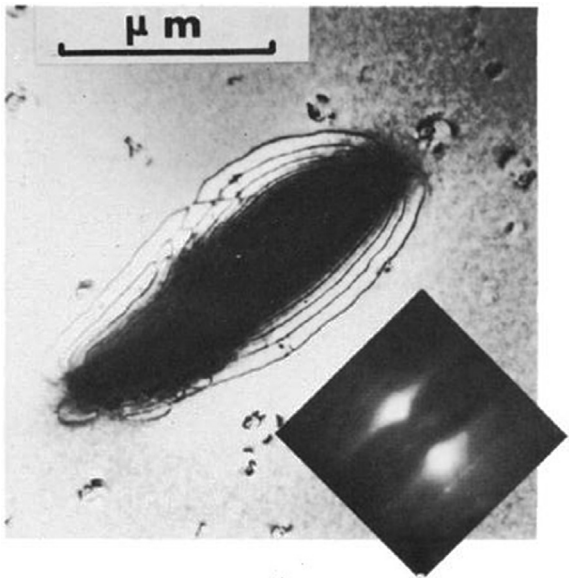

Fig. 2. SEM image of dislocation loops around hydride taken by Carpenter et al. [59].

increased and connectivity and size of hydrides changed drastically, becoming larger and more connected [58]. These studies also found a distinct x-ray diffraction pattern on reoriented hydrides. Further research could be done on the conditions required for hydride orientation, such that procedures can be established for handling used fuel rods that minimize reorientation.

2.4. Mechanical effects of hydrides

Hydrides are known to be extremely brittle at all temperatures [62]. Simpson and Cann found that the strength of the α-Zr matrix has a strong effect on the toughness of Zr–Zr hydride two phase mixtures [62]. They came to the conclusion that improvement in fracture toughness of Zr-2.5 wt% Nb above 150 °C is more related to the reduction in the yield stress of the Zr phase than to any improvement in the hydride phase; because, the lower yield stress of the Zr phase prohibits reaching any stress level large enough to fracture the hydride phase. A recent study by Kubo et al. [63] found that ductile fracture occurs above 200 °C, because of a lower ultimate tensile strength of the Zr matrix, which confirms the work done previously by Simpson and Cann [62]. The ductile to brittle transition temperature of Zr has been shown to be directly correlated to the precipitation of hydrides by Huang and Ho [64], and although brittle fracture at room temperature was only seen in Zr with over 2000 ppm of H, a noticeable loss of ductility was seen starting at very low H concentrations by Bertolino et al. [65].

In a review on environmentally induced cracking of Zr alloys, Cox mentioned that DHC has the largest economic impact of any of the Zr alloy failure processes [66]. He also stated that unlike DHC in Titanium alloys, DHC in Zr can only occur through hydride precipitates. In 1980, Cann and Sexton [67] showed that hydrides tend to form near crack tips, and then they fracture to increase the crack size, leading to the formation of new hydrides on the new tip and repeating the process. This again shows that DHC in Zr can only occur through hydride precipitation. In 1989, Eadie and Ellyin [68] found that hydride precipitation in a plastic zone at a crack tip leads to a compressive zone just at the crack tip and extends the tensile plastic zone past the crack tip significantly. The compressive zone at the crack tip would suppress fracture, which also helps to explain why hydrides at a crack tip exhibit higher fracture toughness than bulk hydrides.

The tensile zone could explain why hydrides grow to a critical length at crack tips, because H tends to migrate to the tensile strained areas. Singh et al. [69] found that DHC rate increases with increasing temperature, potentially due to the increase in H diffusivity and solubility. Perovic et al. [70] found that the direction of hydride formation could be controlled to some extent in the fabrication process, which can be used to limit the effects of DHC. As mentioned previously, radially oriented hydrides have been shown to be more detrimental to mechanical properties and DHC. Therefore a cladding fabricated to have more circumferential precipitates will have less likelihood of reorienting those hydrides to radial during the transition from wet to dry storage. Perovic et al. also concluded that DHC could be somehow controlled if the retained β phase in Zr could be made to remain stable through a stress relief heat treatment process.

Though much has been learned through experimental work on hydride precipitation in Zr alloys, there are several aspects of the formation, morphology, and evolution of hydride precipitate in Zr that can be elaborated through modeling techniques.

3. Computational study of zirconium hydrides

The versatility and cost effectiveness of computational models have led them to become very important tools in studying nano- and microstructures of materials in the past couple of decades as computational efficiency has improved. Because of the growing importance and interest in computational modeling and its role in designing materials, the remainder of this review will focus on computational modeling techniques applied to Zr hydride. First, atomic or nano scale models will be discussed, and later, the mesoscale models for studying the microstructures of Zr hydrides will be reviewed.

3.1. Study of Zr–H system by atomistic modeling techniques

Density Functional Theory (DFT) based on first principals is a computational modeling method used to study materials at the atomic scale. By using functions of electron densities, DFT is able to study many atomic interactions in a material at a relatively low computational cost, making it an efficient method for studying the interactions between small groups of atoms. Using DFT calculations, Domain et al. [71] were able to confirm that H atoms occupy tetrahedral sites preferentially in low temperature Zr. This is different than most metal-H systems, where H atoms prefer octahedral sites. They also determined that H atoms diffuse along the c axis jumping between tetrahedral and octahedral sites. In another DFT study, Blomqvist et al. [72] determined some of the thermodynamic properties of the three main hydride phases using the structures identified in other papers. They found the elastic constants and free energy of formation at several temperatures as well as the phonon band structures. These results are confirmed in a recent DFT study done by Olsson et al. [73]. In order to calculate the free energies using ab initio models, a statistical approach using the full phonon density of states and the thermal electron excitations was used. The approach is commonly referred to as the quasi-harmonic approximation and the method to calculate free energies is described in detail by Olsson et al. [73]. The chemical driving forces (the change in free energy from α-Zr to precipitate) to precipitate γ and ζ hydrides at several temperatures were compared by Thuinet and Besson, as shown in Fig. 3 [74]. They found that ζ hydrides may nucleate initially due to a lower interfacial energy than that of the γ phase.

Recently, Burr et al. studied the effects of second phase particles on the H absorption of Zr alloys by DFT calculations [75,76]. Their results showed that certain Zr-rich second phase particles, such as Zr_3Fe, Zr_2Ni, Zr_2Cu, and Zr_3Sn, provide lower energy sites for H accommodation. This conclusion would indicate that these precipitates could potentially be used as H sinks and decrease the H availability for hydriding. They also found that more common second phase particles such as Zr_2(Fe, Ni) in Zircaloy-2 and β-(Zr, Nb) precipitates have a H affinity similar to α-Zr, and would not work well as H getters. $Zr(Cr, Fe)_2$ found in Zircaloy-4 would be unlikely to accommodate any H, because the solution enthalpies are much higher than those of α-Zr. This suggests that though Zircaloy-4 exhibits a lower H pick-up fraction than Zircaloy-2, it is not due to second phase particles. The lower Ni content of Zircaloy-4 leads to lower H pick-up, though the reason for this is still not well understood.

DFT is useful for studying crystal structure and properties in the nanoscale, but to include more than just a few hundred atoms another approach must be used. The next scale up from DFT is Molecular Dynamics (MD), which while still nanoscale, allows thousands of atoms to be simulated. There have been very few studies done on Zr hydrides through MD because there are not currently very good interatomic potentials for the Zr–H system; Noordhoek et al. recently made one that works for hydrides [77], others made for the Zr–H system do not work as well [78–80]. Zhu et al. completed a study in 2010 on the ductility of the four hydride phases [81]. Their research indicated that the ζ and γ phase hydrides are actually more ductile than α-Zr, while the other two are significantly more brittle, δ phase being the worst. They also found that all four phases have negative formation enthalpies at ambient pressure indicating that all four phases are thermodynamically

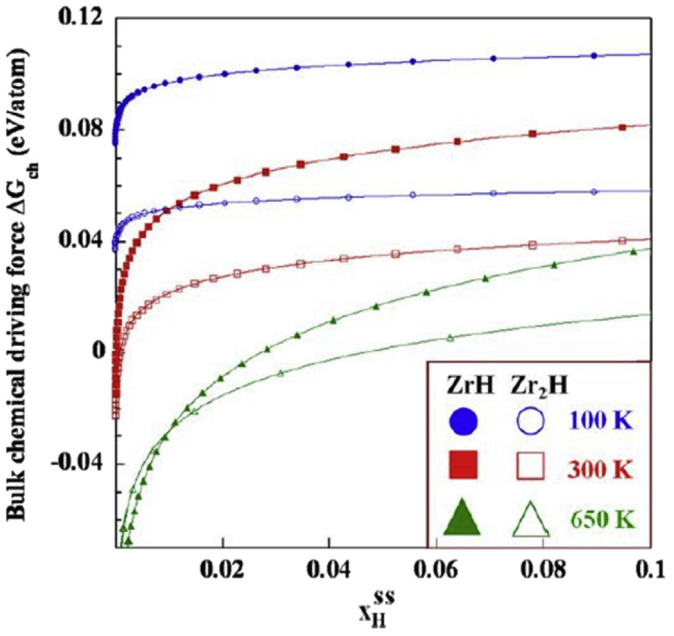

Fig. 3. DFT simulation comparing the driving force for precipitation of two hydride phases from Thuinet and Besson [74]. x_H^{ss} is the amount of H in solid solution.

stable. Only the δ phase was found to be stable for all of the pressure range studied. Their conclusion that δ hydrides are the most brittle phase is supported by a DFT study done by Udagawa et al. [82], who found that δ hydrides are more prone to brittle fracture than iridium, which is an extremely brittle material.

MD was also recently used to simulate H diffusion in Zr hydrides at temperatures between 1000 K and 6000 K by Yanilkin [83]. In this work, an Arrhenius equation relating the diffusion of H to temperature was developed. Lower temperature diffusion rates as well as some material properties such as stiffness constants and lattice parameters were studied in 2012 by Siripurapu et al. [84]. They found that the diffusion of H differs in different directions, being higher along the $[11\bar{2}0]$ and $[01\bar{1}0]$ directions. Diffusion coefficients were also higher under compressive strain than tensile strain.

In order to continue improving the other higher scale models, DFT calculations at different temperatures (commonly called ab initio MD – AIMD) can be used to determine important factors influencing the hydride precipitation and growth, such as stable crystal structures of hydrides at different temperatures, and interfacial energies between different type of hydrides and the matrix of different phases.

3.2. Finite element modeling of DHC

The Finite Element Method (FEM) has been used to solve kinetic models of DHC propagation in the microscale. FEM has been proven as a powerful tool for solving the complex equations of cracking over a micro scale area, by breaking the domain down into many smaller sub-domains and solving for the primary variables iteratively. DHC has been extensively studied by various methods, and there are currently two differing views for its origins, each of which has been modeled using FEM by different researchers. The first view was originally suggested by Dutton and Puls [85–87], which states that DHC is caused by the stress driven flow of H to a crack tip, leading to the formation of hydrides, and these hydrides fracture when a critical length is reached creating a new tip for the process to start again. This view has recently been called the Diffusion First Model [87]. The other view for the origin of DHC was developed by Kim et al. [88,89] over the past fifteen years claiming that DHC happens when hydrides form in stressed regions such as crack tips, creating a difference in concentration of H between stressed and unstressed regions. This concentration difference is the driving force outlined by Kim for the growth of hydrides to the critical length. McRae et al. [87] recently called this view the Precipitation First Model.

Dutton and Puls developed a model which assumes that the average crack velocity is equal to the growth rate of the hydride at the crack tip. The growth of the hydride at the crack tip is related to the flow of H to the crack tip, which is driven by the action of the stress gradient at the crack tip. This original model did not account for the fact that the DHC propagation is intermittent, because the hydride only fractures when it reaches the critical size, and then must again grow to the critical size once the crack propagates [90]. Several models have been made based on the original Diffusion First Model. The most recent version of this model was developed in 2010 by McRae et al. [87], where FEM was used to solve the following equations:

$$J = -D\left(\nabla C + \frac{C}{RT}\nabla\mu^o + \frac{C}{\gamma}\nabla\gamma\right), \tag{1}$$

and

$$\nabla J = -\frac{\partial C}{\partial t}, \tag{2}$$

with a crack velocity of,

$$\nu_c(T) = \frac{k(T)2\pi D}{\varphi}\exp\left[\frac{\mu^o(b)-\mu^o(0)}{RT}\right]\times\left[C(b)\gamma(b) - C(a)\gamma(a)\exp\left[\frac{\mu^o(a)-\mu^o(b)}{RT}\right]\right]. \tag{3}$$

In the above equation, J is the flux of H, μ^o is an arbitrarily assigned reference state chemical potential defined as the bottom of the potential well in which H sits in solid solution (which is dependent on stress), C is the concentration of H in solid solution, γ is the activity coefficient, a and b are the inner and outer radii of the cylinder, k is a proportionality constant, φ is related to the potential and radius of the crack, and R and T are the ideal gas constant and temperature, respectively.

Kim et al. [88,89] in recent years has provided an alternative model claiming that the previous view on the origin of DHC has flaws in several ways. They claim that H diffusion from the bulk to the crack tip under the stress gradient is not possible in a closed system such as the Zr–H system, where H would be unable to move from the bulk to the crack tip without a concentration gradient. Their alternative model claims that the first step in DHC is the precipitation of hydrides at the crack tip when stresses cause the temperature of precipitation to rise and the concentration of precipitation (C_p) to decrease. Then once the hydride has precipitated, a concentration gradient between the bulk and the hydride is created. This gradient draws more H to the crack tip, since the crack tip has the lower H concentration, increasing the size of the hydride until the critical size is reached. Since the model presented by Kim does not involve a stress gradient, McRae et al. [87] presented the flux equation for Kim's model, which is the following equation:

$$J = -D\nabla C, \tag{4}$$

and the crack velocity becomes:

$$\nu_c(T_t) = \frac{k(T_t)2\pi D}{\ln\left(\frac{b}{a}\right)}(C(b)-C(a)). \tag{5}$$

More detailed explanations of the mathematics involved in both models can be found in the paper by McRae et al. [87].

A thorough review of the results of the original model of Dutton and Puls as well as the newer model presented by Kim is provided by Puls in Ref. [86] with full mathematical expressions and arguments for why the Diffusion First Model is better suited for the task of modeling DHC. McRae et al. came to a similar conclusion in their work in 2010 [87], stating that no experimental evidence has been found to date indicating any lowering of C_p due to tensile stress. Without a decrease in C_p, the model proposed by Kim would be impossible. However, in 2010, Kim published a paper again criticizing the original model, stating its flaws and showing that there is still no definite conclusion as to which model is more accurate [89].

Kinetics models, such as those presented in the section, are useful in studying the possible mechanisms of the DHC reaction. However, these models cannot simulate the nucleation, evolution, and morphology of the hydrides, which lead to cracking, and a more advanced mathematical model combining the thermodynamics and kinetics is necessary.

3.3. Phase field modeling of hydride precipitates

A powerful computational modeling technique capable of simulating unstable and stable microstructures of materials is the phase field method. In recent years, γ hydride precipitation has been simulated through phase field modeling by different researchers [4,91–97]. The phase field models use conserved and/or non-conserved field variables, which are continuous across interface regions between phases, to simulate the evolution of composition and/or crystal structure over the spatial domain, respectively [98,99]. The conserved and non-conserved field variables are controlled and evolved by applying temporal and spatial evolution, governed by the Cahn–Hilliard non-linear diffusion equation and the Ginzburg–Landau relaxation equation, respectively. The coupling of these equations minimizes the total free energy of the system. A thorough review of the Landau theory of phase transformation and Ginzburg–Landau theory can be found in Mamivand et al. on phase field modeling martensitic phase transformations [100]. A conceptual background of the phase field method and general advances in this field were presented by Emmerich [101] in 2008, and a thorough review article about the phase field method in relation to microstructure evolution was written in 2008 by Moelans et al. [102]. Phase field models require fundamental thermodynamic and kinetic data from either experiments or atomistic models. With these parameters, a phase field model is able to predict the morphology and microstructure of a material system without explicitly tracking the interface positions [103,104]. This predictive capacity of the phase field method makes it an attractive supplement to expensive experimental studies, as well as a critical modeling scale up from DFT and MD simulations.

The free energy used in the two-dimensional (2D) phase field models of γ hydride precipitation by Shi et al. [105]and others [92–95,97] is as follows:

$$F = F_C + F_{el}, \tag{6}$$

where, F_C is the chemical free energy, and F_{el} is the elastic energy as follows:

$$F_c = \int \left[f(C,\eta_p) + \sum_{p=1}^{v} \frac{\alpha_p}{2}(\nabla\eta_p)^2 + \frac{\beta}{2}(\nabla C)^2 \right] d^3r, \tag{7}$$

$$\begin{aligned} f(C,\eta_p) = {} & \frac{A_1}{2}(C-C_1)^2 + \frac{A_2}{2}(C-C_2)\sum_{p}^{v}\eta_p^2 - \frac{A_3}{4}\sum_{p}^{v}\eta_p^4 \\ & + \frac{A_4}{6}\sum_{p}^{v}\eta_p^6 + A_5\sum_{p\neq q}^{v}\eta_p^2\eta_q^2 + A_6\sum_{p\neq q,r}^{v}\eta_p^4\left(\eta_q^2+\eta_r^2\right) \\ & + A_7\sum_{p\neq q\neq r}^{v}\eta_p^2\eta_q^2\eta_r^2, \end{aligned} \tag{8}$$

In Eq. (7) and Eq. (8), η_p represents the order parameters for each of the three orientations of γ hydride precipitates possible for a 2D model in the basal plane, C is the concentration of H, C_1 and C_2 are the concentration of H in the matrix and precipitate, respectively, α_p and β are the gradient energy coefficients, and A_1 to A_7 are constants. Eqs. (6)–(8) are used in several dimensionless phase field modeling studies of hydride precipitation in Zr alloys. Zhong and Macdonald determined the Gibb's free energy of formation of γ hydrides as a function of temperature in 2012 [106], this could be used to improve the phenomenological free energy functional created by Shi et al. in future studies. For the elastic energy, F_{el}, several variations of Khachaturyan's theory have been used similar to that shown in Eq. (9) [107,108]. These models have used transformation strains and H diffusion strains determined by experiments, such as those found by Carpenter et al., in 1973 [59], and the elastic constants of Zr to define the elastic portion of the free energy equation.

$$\begin{aligned} E_{el} = {} & \frac{V}{2}C_{ijkl}\bar{\varepsilon}_{ij}\bar{\varepsilon}_{kl} - VC_{ijkl}\bar{\varepsilon}_{ij}\sum_{p}^{v}\varepsilon_{kl}^{0}(p)\eta_p^2(r) + \frac{V}{2}C_{ijkl}\sum_{p}^{v} \\ & \times \sum_{q}^{v}\varepsilon_{ij}^{0}(p)\varepsilon_{kl}^{0}(q)\eta_p^2(r)\eta_q^2(r) - \frac{1}{2}\sum_{p}^{v} \\ & \times \sum_{q}^{v}\int \frac{d^3g}{(2\pi)^3}B_{pq}(n)\left\{\eta_p^2(r)\right\}_g^*\left\{\eta_q^2(r)\right\}_g \end{aligned} \tag{9}$$

Each of these models has used the Ginzburg–Landau and Cahn–Hilliard governing equations as follows:

$$\frac{\partial\eta_p}{\partial t} = -L_p\frac{\partial F}{\partial\eta_p} + noise, \tag{10}$$

$$\frac{\partial C}{\partial t} = M\nabla^2\frac{\partial F}{\partial C} + noise, \tag{11}$$

where L_p and M are the structural relaxation and diffusional mobility coefficients respectively.

The first phase field models created for this system were simple single grain non-dimensional maps of the growth shape and direction of γ hydrides with and without a uniform applied load; there was no relation between the models and actual physical domains and properties, and these models were only used to study morphology phenomenologically. A representation of the results from these first models are shown in Fig. 4 [91].

Some other dimensionless phase field modeling studies using a similar free energy have also been done for bicrystalline Zr [92], for non-uniform applied loads [93], and for a specimen with flaws such as a crack [94,95]. Modeling of cracks was accomplished through adding plasticity to previous models driven by a reduction in distortion strain energy using a variation on the classic Prandtl Reuss theory [109]. Some assumptions were made to accomplish the addition of plastic deformation: no plastic deformation was considered within hydride precipitates, and the plastic strain during nucleation of hydrides was zero throughout the system.

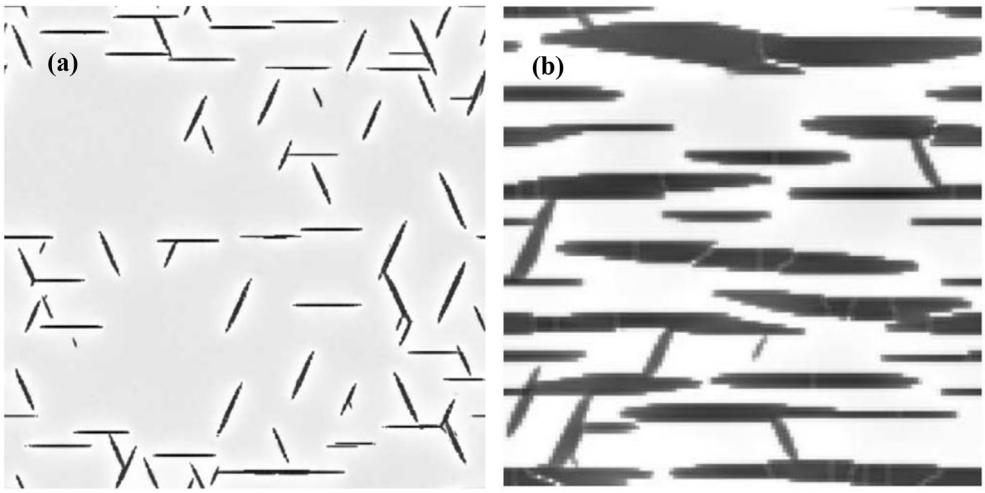

Fig. 4. a) Random seeded γ hydride growth in all three orientations in a unitless 512 × 512 grid. b) Vertically applied tensile strain causes hydrides to grow preferentially in the horizontal orientation in 128 × 128 unit-less grid [91].

Distortion strain energy was derived based on the deviatoric strain rather than the stress free strain. Evolution of the plastic zone is solved using the following Langevin equation:

$$\frac{\partial \varepsilon_{ij}^{p}(r_p,t)}{\partial t} = -N_{ijkl}\frac{\partial E^{dis}}{\partial \varepsilon_{kl}^{p}(r_p,t)}, \tag{12}$$

where N_{ijkl} is a kinetic coefficient characterizing the structural evolution rate of plastic deformation, E^{dis} is the distortion strain energy, and ε_{ij}^{p} is the plastic strain. The results of these simulations were in qualitative agreement with the results from experimental studies, showing hydride preference for growth near grain boundaries and growth perpendicular to applied strain. However, they were unable to show real time and length scales, and also were lacking any temperature change.

Shi and Xiao have recently completed a phase field study with a temperature dependent model of single grain γ hydrides, although some key parameters including interface energy between hydride and matrix, temperature gradient, and adding the δ phase are still lacking [105]. This phase field model also still has several phenomenological parameters in the Landau free energy polynomial used to develop the model. While it has room for improvement, this most recent model is able to compare relatively well with experimental hydride lengths found by Bailey [5]. Their simulation results are shown with Bailey's experimental results in Fig. 5; the average length of the hydrides in the simulation was 1.18 μm and in the experiment it was 1.31 μm.

The evolution of the more recently discovered ζ phase has been simulated by Thuinet et al. using only the Cahn–Hilliard equation, without including the Ginzburg–Landau equation [96,110]. Due to the fact that there is only one eigenstrain for ζ phase precipitates, no non-conserved order parameters are necessary to simulate the precipitation of ζ phase. The three orientations of the ζ phase precipitates come from the inhomogeneity of elastic constants between the precipitates and the matrix. The elastic tensors of the phase field must then be calculated iteratively which increases the computational time. This method has been proven to be effective in several studies on microstructures with significant elastic inhomogeneities [111–113]. Results of Thuinet et al. simulations indicate a high dependence of morphology of ζ hydrides on the C_{15} coefficient in the trigonal stiffness matrix. They found that their results could not be duplicated using homogeneous stiffness matrices, creating simple circles rather than the observed rods. The apparent dependence of ζ hydrides on the inhomogeneous stiffness is interesting because phase field models of γ hydride growth have indicated that expected rod shape of γ hydrides is predicted by the eigenstrains and using homogeneous stiffness matrices [92–95,105,114]. Thuinet et al. model uses a double well chemical free energy equation as follows:

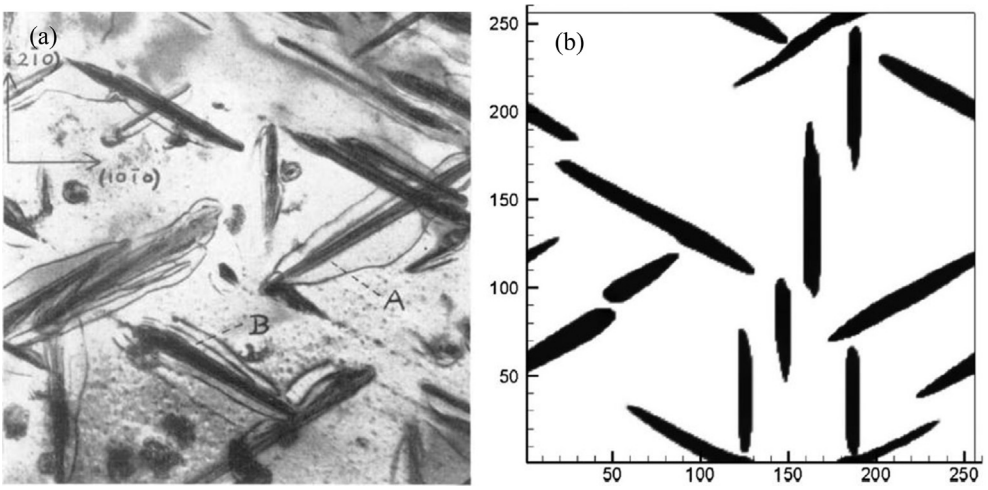

Fig. 5. SEM image of γ hydrides done by Bailey [5] (a) and quantitative phase field simulation results by Shi and Xiao [105] (b). The side length on both images is around 4 μm.

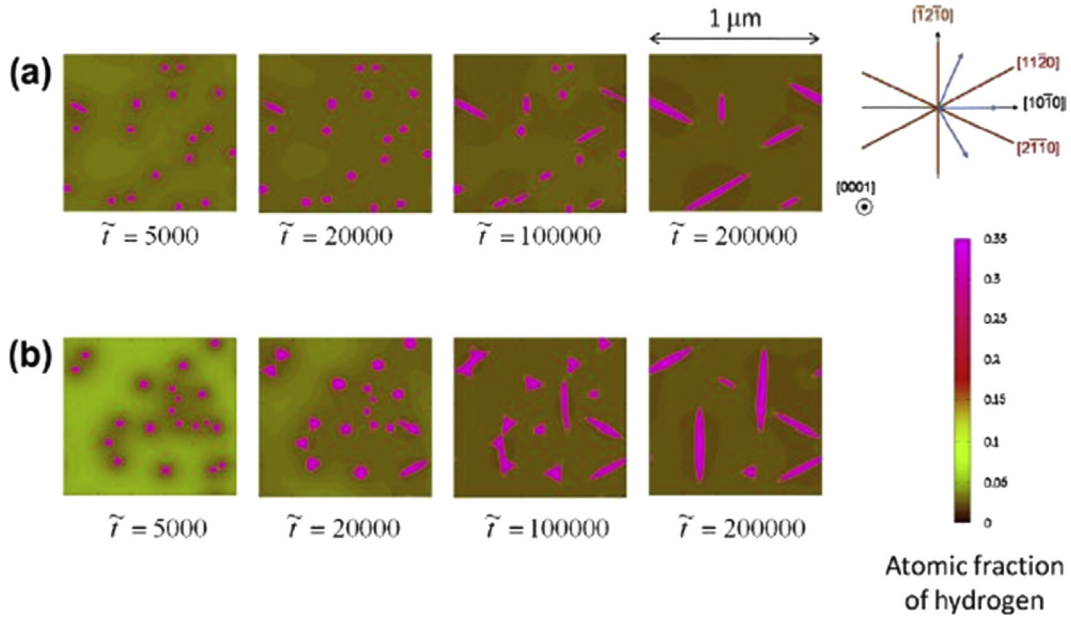

Fig. 6. a) Evolution of ζ hydrides without any applied stress at 4 at % H and b) 5 at % [96].

$$f_{\text{hom}}(c) = A\left[-\frac{1}{2}(c(r,t)-\bar{c})^2 + \frac{1}{\Delta c^2}(c(r,t)-\bar{c})^4\right], \quad (13)$$

where $\bar{c}$ is $\frac{c_1+c_2}{2}$, Δc is the difference between phase concentrations, and A is the free energy scale parameter. Other equations used in the model are similar to those used in simulating γ hydrides. Thuinet et al. were able to use interfacial energies from their ab initio studies previously done for ζ hydrides [74]. Their simulations show similar results for the ζ hydrides as were found for γ hydrides in relation to applied strain. Fig. 6 shows ζ hydrides growth with no applied strain at different H concentrations. Simulations were also done with an applied stress which reoriented the hydrides as expected.

All of the mentioned phase field models simulating γ or ζ precipitates, with the exception of the recent model by Shi and Xiao [105], have been non-dimensional isothermal phenomenological models. These models are useful only for the purpose of understanding the shape evolution of hydrides, and they cannot provide the actual size or time dependent evolution of hydride precipitates. The model by Shi and Xiao is also missing some key parameters necessary to improve its accuracy and should also be improved to involve temperature gradient so that simulations could be done for actual operating and storage environments.

Phase field modeling could also be used to shed light on the argument between different theories about how DHC occurs. Since the phase field model is coupled to the constitutive equations of mechanical behavior of the material, at any point in time, it determines the maps of stress and H concentration for the entire modeling domain. By introducing an initial crack in the model, the model can be used to see what the first step of DHC is. Experimental work should be used simultaneously to verify each progressing model and potentially provide more accurate material parameters to improve the models.

4. Conclusion

In this article, we reviewed both experimental and computational studies on the formation and growth of hydrides in Zr alloys. Experimental research has provided important information about the structure of hydrides, their formation and reorientation, solubility and absorption of H, and the effects of DHC on cladding materials. However, there is still much to be learned. H absorption rate is crucial to the lifetime of claddings, and further research should be done to investigate the possible alloying elements or precipitates (such as those identified as possibilities in the DFT work by Burr et al. [75]) that can be used to reduce absorption. The current experimental work has not provided a clear understanding of habit planes, or a definite conclusion on the stability of γ hydrides. These longstanding debates should be studied further to determine what may have caused a δ to γ phase transformation, as well as a possible temperature effect on habit planes. Grain boundaries may also play a significant role in the growth of hydrides, and further studies are needed to determine energies, orientations, and other important data which could promote or halt hydride precipitation. It is also important to better understand the possible factors that control reorientation of hydrides; this understanding will help to reduce the risk of reorientation of hydrides to the radial direction during the transition of used fuel rods to storage.

Existing experimental data on hydride precipitation in Zr alloys provide an important foundation to improve the development of quantitative computational methods for accurate prediction of the formation and evolution of hydrides, and also elucidating the mechanics of DHC. Future experimental data is necessary to provide important thermodynamic and kinetic information by the simulation approaches, and also to verify the computational results.

There are a few computational works on hydride precipitation in Zr and Zr alloys. At the electronic scale, DFT calculations were used to verify H occupation sites, free energies of different phases, H absorption, and some other important phenomena. At the atomistic scale, MD simulations were used to find H diffusion in precipitates. At the mesoscale, some models have been created to simulate DHC, and phase field models have been developed to qualitatively simulate hydride growth and morphology of the ζ and γ phases. Further atomistic modeling efforts need to be undertaken to provide unknown interfacial energies of the hydride–hydride and hydride-Zr interfaces, grain boundary energies of polycrystalline Zr and Zr alloys which can be influenced by H concentration, and the mobility coefficients. These are necessary input data for mesoscale models of hydride microstructural evolution, such as phase field models. Once these data are obtained, mesoscale phase field models could be created which do not use any phenomenological

parameters. Current phase field models developed to study hydride precipitation in Zr alloys are mostly phenomenological models considering isothermal conditions, which cannot simulate the actual size or time dependent evolution of hydride precipitates. The free energy functional of the phase field models needs to be connected to the thermodynamics and temperature-dependent formation energy of different phases. This will enable simulating hydride precipitation in a temperature gradient, as well as the formation of both γ and δ phases in a single model.

Acknowledgment

This work was supported by Idaho National Laboratory Directed Research and Development funds.

References

[1] A. Zielinski, S. Sobieszczyk, Int. J. Hydrogen Energy 36 (2011) 8619–8629.
[2] K. Une, S. Ishimoto, J. Nucl. Mater. 322 (2003) 66–72.
[3] M.P. Puls, The Effect of Hydrogen and Hydrides on the Integrity of Zirconium Alloy Components, Springer, London, 2012.
[4] Z. Zhao, M. Blat-Yrieix, J.-P. Morniroli, A. Legris, L. Thuinet, Y. Kihn, A. Ambard, L. Legras, J. ASTM Int. 5 (2008) 1–20.
[5] J.E. Bailey, Acta Metall. 11 (1963) 267–280.
[6] G.J.C. Carpenter, Acta Metall. 26 (1978) 1225–1235.
[7] L.D.L. Grange, L.J. Dykstra, J.M. Dixon, U. Merten, J. Phys. Chem. 63 (1959) 2035–2041.
[8] G.G. Libowitz, J. Nucl. Mater. 5 (1962) 228–233.
[9] K.E. Moore, W.A. Young, J. Nucl. Mater. 27 (1968) 316–324.
[10] K.E. Moore, J. Nucl. Mater. 32 (1969) 46–56.
[11] W.E. Wang, D.R. Olander, J. Am. Ceram. Soc. 78 (1995) 3323–3328.
[12] E. Zuzek, Surf. Coat. Technol. 28 (1986) 323–338.
[13] E. Zuzek, J.P. Abriata, Bull. Alloy Phase Diagr. 11 (1990) 385–395.
[14] K.G. Barraclough, C.J. Beevers, J. Nucl. Mater. 34 (1970) 125–134.
[15] S. Mishra, K. Sivaramakrihnan, M. Asundi, J. Nucl. Mater. 45 (1972) 235–244.
[16] J.H. Root, W.M. Small, D. Khatamian, O.T. Woo, Acta Mater. 51 (2003) 2041–2053.
[17] A. Steuwer, J. Santisteban, M. Preuss, M. Peel, T. Buslaps, M. Harada, Acta Mater. 57 (2009) 145–152.
[18] K. Barraclough, C. Beevers, J. Less Common Metals 35 (1974) 177–179.
[19] E. Tulk, M. Kerr, M.R. Daymond, J. Nucl. Mater. 425 (2012) 93–104.
[20] L. Lanzani, M. Ruch, J. Nucl. Mater. 324 (2004) 165–176.
[21] A. Barrow, A. Korinek, M. Daymond, J. Nucl. Mater. 432 (2013) 366–370.
[22] G.F. Slattery, J. Nucl. Mater. 32 (1969) 30–38.
[23] W.H. Erickson, D. Hardie, J. Nucl. Mater. 2 (1964) 254–262.
[24] A. Sawatzky, B.J.S. Wilkins, J. Nucl. Mater. 22 (1967) 304–310.
[25] M.P. Puls, Acta Metall. 29 (1981) 1961–1968.
[26] K. Une, S. Ishimoto, Y. Etoh, K. Ito, K. Ogata, T. Baba, K. Kamimura, Y. Kobayashi, J. Nucl. Mater. 389 (2009) 127–136.
[27] K.B. Colas, A.T. Motta, J.D. Almer, M.R. Daymond, M. Kerr, A.D. Banchik, P. Vizcaino, J.R. Santisteban, Acta Mater. 58 (2010) 6575–6583.
[28] C.D. Cann, A. Atrens, J. Nucl. Mater. 88 (1980) 42–50.
[29] C.E. Ells, J. Nucl. Mater. 28 (1968) 129–151.
[30] G.J.C. Carpenter, J.F. Watters, J. Nucl. Mater. 73 (1978) 190–197.
[31] A. Couet, A.T. Motta, R.J. Comstock, R.L. Paul, J. Nucl. Mater. 425 (2012) 211–217.
[32] A. Couet, A.T. Motta, R.J. Comstock, J. Nucl. Mater. 451 (2014) 1–13.
[33] S. Kass, J. Electrochem. Soc. 107 (1960) 594–597.
[34] W.E. Berry, D.A. Vaughan, E.L. White, Corrosion 17 (1961) 109t–117t.
[35] Y. Hatano, M. Sugisaki, K. Kitano, M. Hayashi, Special Technical Publication, ASTM 1354 (2000) 901–917.
[36] G.C. Weatherly, Acta Metall. 29 (1981) 501–512.
[37] D.G. Westlake, J. Nucl. Mater. 26 (1968) 208–216.
[38] F.W. Kunz, A.E. Bibb, Trans. Met. Soc. AIME 218 (1960) 133–135.
[39] D.G. Westlake, E.S. Fisher, Trans. Met. Soc. AIME 224 (1962) 254–258.
[40] R.P. Marshall, J. Nucl. Mater. 24 (1967) 49–59.
[41] R.N. Singh, P. Ståhle, L. Banks-Sills, M. Ristinmaa, S. Banerjee, Defect and Diffusion Forum, Trans Tech Publ, 2008, pp. 105–110.
[42] N.K. Kumar, J. Szpunar, Mater. Sci. Eng. A 528 (2011) 6366–6374.
[43] N.K. Kumar, J.A. Szpunar, Z. He, J. Nucl. Mater. 403 (2010) 101–107.
[44] Z. Wang, U. Garbe, H. Li, A.J. Studer, R.P. Harrison, M.D. Callaghan, Y. Wang, X. Liao, Scr. Mater. 67 (2012) 752–755.
[45] Z. Wang, U. Garbe, H. Li, Y. Wang, A.J. Studer, G. Sun, R.P. Harrison, X. Liao, V. Alvarez, J. Santisteban, J. Appl. Crystallogr. 47 (2014) 303–315.
[46] Y.S. Kim, Y. Perlovich, M. Isaenkova, S.S. Kim, Y.M. Cheong, J. Nucl. Mater. 297 (2001) 292–302.
[47] B. Nath, G.W. Lorimer, N. Ridley, J. Nucl. Mater. 58 (1975) 153–162.
[48] J.S. Bradbrook, G.W. Lorimer, N. Ridley, J. Nucl. Mater. 42 (1972) 142–160.
[49] B. Nath, G.W. Lorimer, N. Ridley, J. Nucl. Mater. 49 (1973) 262–280.
[50] C.D. Cann, M.P. Puls, E.E. Sexton, W.G. Hutchings, J. Nucl. Mater. 126 (1984) 197–205.
[51] K. Une, K. Nogita, S. Ishimoto, K. Ogata, J. Nucl. Sci. Technol. 41 (2004) 731–740.
[52] V.S. Arunachalam, B. Lehtinen, G. Ostberg, J. Nucl. Mater. 21 (1967) 241–248.
[53] K.V.M. Krishna, A. Sain, I. Samajdar, G.K. Dey, D. Srivastava, S. Neogy, R. Tewan, S. Banerjee, Acta Mater. 54 (2006) 4665–4675.
[54] K.V.M. Krishna, D. Srivastava, G.K. Dey, V. Hiwarkar, I. Samajdar, S. Banerjee, J. Nucl. Mater. 414 (2011) 270–275.
[55] M.P. Puls, Metall. Trans. A 22A (1991) 2327–2337.
[56] C.J. Beevers, D.V. Edmonds, J. Nucl. Mater. 33 (1969) 107–113.
[57] W. Qin, N.K. Kumar, J. Szpunar, J. Kozinski, Acta Mater. 59 (2011) 7010–7021.
[58] K.B. Colas, A.T. Motta, M.R. Daymond, J.D. Almer, J. Nucl. Mater. 440 (2013) 586–595.
[59] G.J.C. Carpenter, J.F. Watters, R.W. Gilbert, J. Nucl. Mater. 48 (1973) 267–276.
[60] K.B. Colas, A.T. Motta, M.R. Daymond, M. Kerr, J.D. Almer, J. ASTM Int. 8 (2011).
[61] K. Colas, A. Motta, M.R. Daymond, J. Almer, in: ASTM 17th International Symposium on Zirconium in the Nuclear Industry, 2013, pp. 1107–1137.
[62] L.A. Simpson, C.D. Cann, J. Nucl. Mater. 87 (1979) 303–316.
[63] T. Kubo, Y. Kobayashi, H. Uchikoshi, J. Nucl. Mater. 435 (2013) 222–230.
[64] J.H. Huang, C.S. Ho, Mater. Chem. Phys. 38 (1994) 138–145.
[65] G. Bertolino, G. Meyer, J.P. Ipina, J. Nucl. Mater. 320 (2003) 272–279.
[66] B. Cox, J. Nucl. Mater. 170 (1990) 1–23.
[67] C.D. Cann, E.E. Sexton, Acta Metall. 28 (1980) 1215–1221.
[68] R.L. Eadie, F. Ellyin, Scr. Metall. 23 (1989) 585–592.
[69] R.N. Singh, N. Kumar, R. Kishore, S. Roychaudhury, T.K. Sinha, B.P. Kashyap, J. Nucl. Mater. 304 (2002) 189–203.
[70] V. Perovic, G.C. Weatherly, C.J. Simpson, Acta Metall. 31 (1983) 1381–1391.
[71] C. Domain, R. Besson, A. Legris, Acta Mater. 50 (2002) 3513–3526.
[72] J. Blomqvist, J. Olofsson, A.-M. Alvarez, C. Bjerkén, arXiv preprint arXiv: 1211.0858, (2012).
[73] P. Olsson, A. Massih, J. Blomqvist, A.-M. Alvarez Holston, C. Bjerkén, Comput. Mater. Sci. 86 (2014) 211–222.
[74] L. Thuinet, R. Besson, Intermetallics 20 (2012) 24–32.
[75] P.A. Burr, S.T. Murphy, S.C. Lumley, M.R. Wenman, R.W. Grimes, Corros. Sci. 69 (2013) 1–4.
[76] P.A. Burr, S.T. Murphy, S.C. Lumley, M.R. Wenman, R.W. Grimes, J. Nucl. Mater. 443 (2013) 502–506.
[77] M.J. Noordhoek, T. Liang, T.-W. Chiang, S.B. Sinnott, S.R. Phillpot, J. Nucl. Mater. 452 (2014) 285–295.
[78] A.C. van Duin, B.V. Merinov, S.S. Jang, W.A. Goddard, J. Phys. Chem. A 112 (2008) 3133–3140.
[79] S. Liu, S. Shi, H. Huang, C. Woo, J. Alloys Compd. 330 (2002) 64–69.
[80] M. Ruda, D. Farkas, J. Abriata, Phys. Rev. B 54 (1996) 9765.
[81] W. Zhu, R. Wang, G. Shu, P. Wu, H. Xiao, J. Phys. Chem. 114 (2010) 22361–22368.
[82] Y. Udagawa, M. Yamaguchi, H. Abe, N. Sekimura, T. Fuketa, Acta Mater. 58 (2010) 3927–3938.
[83] A. Yanilkin, Phys. Solid State 56 (2014) 1879–1885.
[84] R.K. Siripurapu, J.A. Szpunar, B. Szpunar, in: PRICM: 8 Pacific Rim International Congress on Advanced Materials and Processing, Wiley Online Library, 2013, pp. 3119–3126.
[85] R. Dutton, M.P. Puls, TMS-AIME, New York, (1976), pp. 512–525.
[86] M.P. Puls, J. Nucl. Mater. 393 (2009) 350–367.
[87] G.A. McRae, C.E. Coleman, B.W. Leitch, J. Nucl. Mater. 396 (2010) 130–143.
[88] Y.S. Kim, S.B. Ahn, Y.M. Cheong, J. Alloys Compd. 429 (2007) 221–226.
[89] Y.S. Kim, J. Nucl. Mater. 396 (2010) 144–148.
[90] R. Dutton, K. Nuttall, M.P. Puls, L.A. Simpson, Metall. Trans. A 8A (1977) 1553–1562.
[91] X.Q. Ma, S.Q. Shi, C.H. Woo, L.Q. Chen, Comput. Mater. Sci. 23 (2002) 283–290.
[92] X.Q. Ma, S.Q. Shi, C.H. Woo, L.Q. Chen, Scr. Mater. 47 (2002) 237–241.
[93] X.Q. Ma, S.Q. Shi, C.H. Woo, L.Q. Chen, Mech. Mater. 38 (2006) 3–10.
[94] X.H. Guo, S.Q. Shi, Q.M. Zhang, X.Q. Ma, J. Nucl. Mater. 378 (2008) 110–119.
[95] X.H. Guo, S.Q. Shi, Q.M. Zhang, X.Q. Ma, J. Nucl. Mater. 378 (2008) 120–125.
[96] L. Thuinet, A.D. Backer, A. Legris, Acta Mater. 60 (2012) 5311–5321.
[97] X.Q. Ma, S.Q. Shi, C.H. Woo, L.Q. Chen, Mater. Sci. Eng. A 334 (2002) 6–10.
[98] M.A. Zaeem, H.E. Kadiri, S.D. Mesarovic, M.F. Horstemeyer, P. Wang, J. Phase Equilib. Diffus. 32 (2011) 302–308.
[99] M.A. Zaeem, S.D. Mesarovic, J. Comput. Phys. 229 (2010) 9135–9149.
[100] M. Mamivand, M.A. Zaeem, H.E. Kadiri, Comput. Mater. Sci. 77 (2013) 304–311.
[101] H. Emmerich, Adv. Phys. 57 (2008) 1–87.
[102] N. Moelans, B. Blanpain, P. Wollants, Comput. Coupling Phase Diagr. Thermochem. 32 (2008) 268–294.
[103] J.Z. Zhu, T. Wang, S.H. Zhou, Z.K. Liu, L.Q. Chen, Acta Mater. 52 (2004) 833–840.
[104] A. Finel, Y.L. Bouar, A. Gaubert, U. Salman, Comptes Rendus Phys. 11 (2010) 245–256.
[105] S.Q. Shi, Z. Xiao, J. Nucl. Mater. 459 (2015) 323–329.
[106] Y. Zhong, D. Macdonald, J. Nucl. Mater. 423 (2012) 87–92.
[107] A.G. Khachaturyan, Theory of Structural Transformations in Solids, Wiley, New York, 1983.
[108] Y.M. Jin, Y.U. Wang, A.G. Khachaturyan, Philos. Mag. 83 (2003) 1587–1626.
[109] J. Chakrabarty, Theory of Plasticity, Butterworth-Heinemann, 2012.
[110] L. Thuinet, A. Legris, L. Zhang, A. Ambard, J. Nucl. Mater. 438 (2013) 32–40.
[111] L. Thuinet, A. Legris, Acta Mater. 58 (2010) 2250–2261.
[112] S. Hu, L. Chen, Acta Mater. 49 (2001) 1879–1890.
[113] G. Boussinot, Y. Le Bouar, A. Finel, Acta Mater. 58 (2010) 4170–4181.
[114] Z. Xiao, M. Hao, X. Guo, G. Tang, S.-Q. Shi, J. Nucl. Mater. 459 (2015) 330–338.